Detection of Abnormal Ionospheric Activity from the EPN and Impact on Kinematic GPS positioning

N. Bergeot, C. Bruyninx, E. Pottiaux, S. Pireaux, P. Defraigne, J. Legrand
Royal Observatory of Belgium

Introduction

The electron content in the ionosphere produces delays in the propagation of radio waves, affecting navigation systems, as well as radio science and radio astronomy. Moreover, GNSS errors due to the ionosphere will increase in the next few years due to the increase of the solar activity since the beginning of the 24th sunspot cycle (early 2008).

To better understand the physics of the ionosphere and its effects on GNSS positioning, the Royal Observatory of Belgium (ROB) is developing an automatic monitoring to detect rapid ionospheric changes in both time and space domains using the data from the EUREF Permanent Network (EPN). To check the ability of the EPN to detect abnormal ionospheric activity we focus on the abnormal ionospheric activity during the Halloween super-storm of 29-31 October 2003.

Firstly, the impact of small-scale ionospheric activity on the coordinate repeatability of kinematic GPS positioning was investigated. Secondly, hourly ionospheric maps were computed and validated by comparing them with the IGS Global Ionosphere Model (GIM). Finally, we investigated a new method to allow the detection of ionospheric heterogeneities at a smaller-scale than possible with the previously obtained ionospheric maps.

1. Impact of the ionosphere on GPS kinematic positioning

Double difference ionosphere-free (L3) GPS phase observables are used to process GPS data in many research applications (e.g. real time kinematic positioning, earthquake monitoring …). To quantify the effect of local variations in the ionospheric state on GPS kinematic positioning we processed 40 GPS stations from the EPN during a period around the 29-31 October 2003 geomagnetic super-storm period (days 292 to 313 of 2003). On 30 October 2003 at 20:07 UT, Fennoscandian experienced a large-scale blackout in Sweden caused by a geomagnetically induced current [*Pulkkinen et al.*, 2005].

1.1 GPS data processing

In a first step, L3 double difference carrier phase observables where used to determine precise daily positions for all stations in a network approach using the Bernese v5.0 software [*Dach et al.*, 2007]. Ambiguities were resolved using the QIF strategy, and the tropospheric refraction was corrected (Wet-Niell mapping function, hourly ZTD corrections, one daily horizontal gradient). In a second step, all stations, except one, were fixed to their estimated positions and 5-minute kinematic positions were estimated for one station in the network. In this stage we used L3 double difference from phase observables, introduced the ambiguities and tropospheric estimates

from the first step, and estimated each 5-minute the residuals with respect to the *a priori* daily coordinates estimated in previous step. This step was repeated for each of the stations separately.
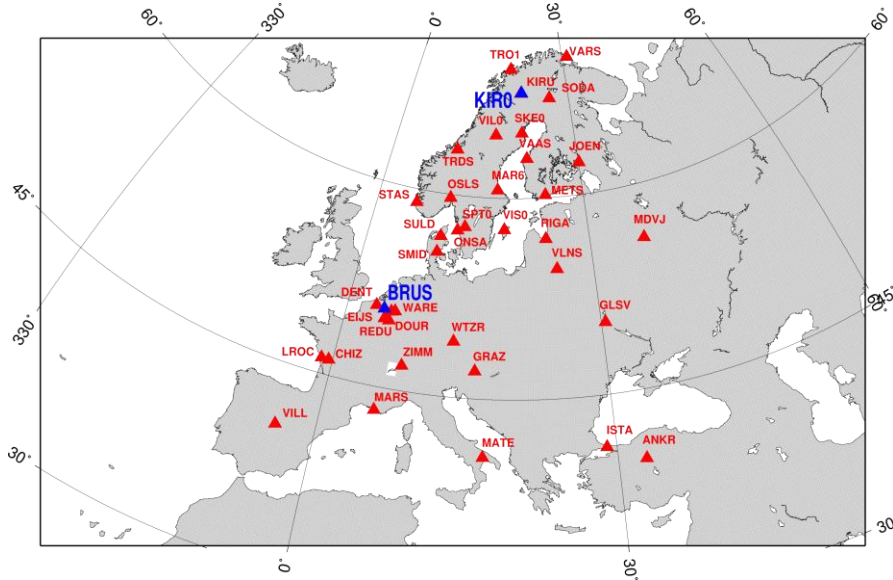
Figure 1: GPS stations processed. The blue stations correspond to the time series in Figure 2.

1.2 Repeatability of Kinematic Coordinates

While the coordinate time series obtained from the 5-minute kinematic positions for the stations BRUS (Brussels, Belgium) is not much affected by the geomagnetic storm, the coordinates of KIR0 (Kiruna, Sweden) have outliers reaching 7.4, 6.6 and 25.2 cm on North, East and Up components respectively (Figure 2).

GPS site	Longitude (°)	Latitude (°)	Hourly repeatability East (cm)		Hourly repeatability North (cm)		Hourly repeatability Up (cm)	
			Min	Max	Min	Max	Min	Max
VARS	31.03	70.34	0.1	2.4	0.1	3.1	0.2	18.2
TRO1	18.94	69.66	0	4.1	0.1	7.5	0.1	28.1
KIR0	21.06	67.88	0	1.9	0.1	2.8	0.1	25.7
KIRU	20.97	67.86	0.1	1.4	0.1	1.6	0.1	10.2
SODA	26.39	67.42	0	2.1	0.1	6.7	0.2	12.9
SKE0	21.05	64.88	0	2	0.1	2.7	0.1	7.1
VILO	16.56	64.7	0	2.7	0.1	2.7	0.1	7.4
TRDS	10.32	63.37	0.1	1.6	0.1	2.6	0.1	5.1
VAAS	21.77	62.96	0.1	1.3	0.1	1.8	0.2	8
JOEN	30.1	62.39	0.1	1.6	0.1	2.6	0.1	13.3
METS	24.4	60.22	0	1.4	0	1.8	0.1	4.2
OSLS	10.37	59.74	0.1	5.9	0.1	11.2	0.2	21
STAS	5.6	59.02	0.1	8	0.1	12.8	0.2	32.8
SPT0	2.89	57.71	0.1	1	0.1	2.2	0.1	4.5
SULD	9.74	56.84	0	1.5	0	1.9	0.1	6.5
BRUS	4.36	50.8	0.1	0.9	0.1	1.9	0.2	2.7
LROC	-1.22	46.16	0.1	1.4	0.1	2.5	0.1	2.7

CHIZ	*-0.41*	*46.13*	0.04	1.02	0.08	2.18	0.08	3

Table 1: Example of minimum and maximum hourly repeatability on East, North and Up components (cm).

In general, stations located in Fennoscandian, where the geomagnetic super-storm influence was maximum [e.g. *Pulkkinen et al.*, 2005], the hourly repeatability of the kinematic positions reaches 5.9, 12.8 and 32.8 cm on the East, North and Up components respectively (Table 1). For stations in central Europe, the repeatability is of the order of few millimetres in the horizontal components and 1 cm in the up component. The degradation of the repeatability is in good accordance with the maximum geomagnetic disturbances activity observed in northern Europe from [*Pulkkinen et al.*, 2005] during that specific geomagnetic super storm.

Consequently, for applications requiring few centimeters precision in kinematic mode during strong ionospheric activity, it is necessary to investigate whether a priori knowledge on the ionosphere can help to reduce the repeatabilities in kinematic GPS positioning.
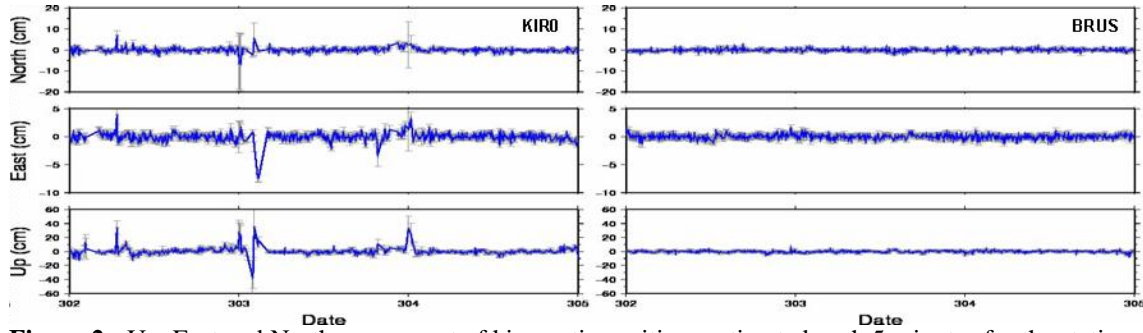

Figure 2 : Up, East and North component of kinematic positions estimated each 5 minutes for the stations BRUS and KIR0 for days 302 to 305 in 2003.

2. Detection of Abnormal Ionospheric Activity from TEC Maps

2.1 GPS Data Processing

We processed the EPN GPS data of the stations indicated in Figure 3 from 22 days in 2003 (days 292 to 313) and 2008 (days 001 to 022) with the Bernese v5.0 software. The strategy adopted is the identical to the one used by the CODE Analysis Center to produce their Global Ionospheric Maps [Schaer et al., 1996].
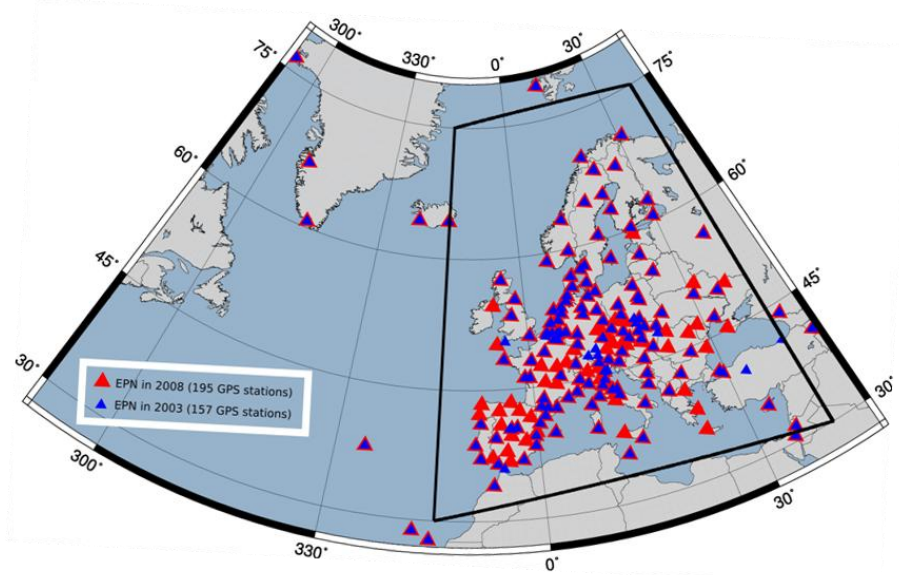
Figure 3: EPN network processed in this study. The black lines delimit the area considered for TEC maps estimation (next sections).

In a first step, a Precise Point Positioning solution using the ionosphere-*free* (L3) code and phase observations was used to estimate stations coordinates, receiver clock corrections as well as station-specific troposphere parameters. In a second step, the zero difference *geometry-free* (L4) code and phase observations (containing only the ionospheric refraction and ambiguity parameters) were used to estimate differential codes biases and the ionospheric model.

For consistency with the IGS final orbits and ERPs, relative antenna phase centre corrections were used before GPS week 1400, and absolute corrections afterwards.

2.2 European Ionospheric Maps

The Total Electron Content maps were estimated using a single layer model in which all free electrons are concentrated in a shell of infinitesimal thickness (450km is considered as the peak height of the electron density profile in the F-region). We developed the surface density of the ionospheric layer into a series of spherical harmonic (*n=m=6*) functions [Schaer et al., 1996] and estimated one model per day. For time domain representation, we applied piece-wise linear functions.

We computed hourly TEC maps for a 1°x1° grid in the IONEX format [Schaer et al., 1998] and focused on the 29-31 October 2003 period with the geomagnetic super-storm. From these maps (Figure 4), we detect an abnormal ionospheric activity characterized by a maximum of 25 TECU located in the North of the Europe. Between 18h and 23h UT, day 303 2003, we estimate a mean of 13 TECU while, during other days (normal ionospheric activity), this mean fluctuates between 3-5 TECU (Figure 4).
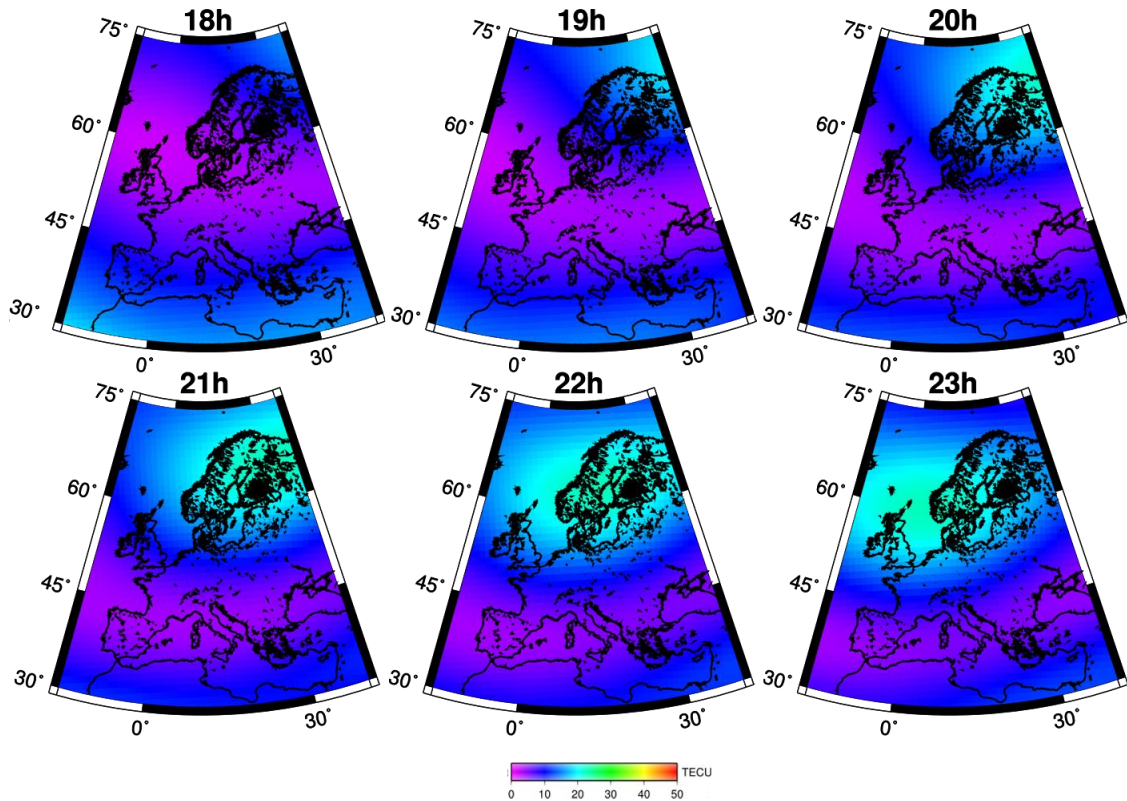
Figure 4: Hourly TEC maps for the 30th, October 2003 (day 303-2003) between 18h and 23h.

2.3 Validation of the TEC maps

Our regional TEC maps have been compared with the Global Ionosphere Maps (GIM) from the CODE analysis center which are computed each 2 hour on a 5/2.5 degree grid in longitude and latitude respectively. After re-sampling our TEC maps to obtain the same resolution as the CODE's GIM, the mean difference (computed over the grid points) between the two TEC maps is below the 1 TECU level. The corresponding RMS is larger during high ionospheric activity (5.2 TECU in Figure 5b) than normal activity (1.9 TECU in Figure 5*a*). Consequently, our results are in good agreement with the GIM during quiet ionospheric activity. However, during the geomagnetic storm period, differences can reach 25 TECU and they are due to the fact that our regional TEC maps allow the detection of TEC variations at smaller scale in time and space domains compared to the GIM products.
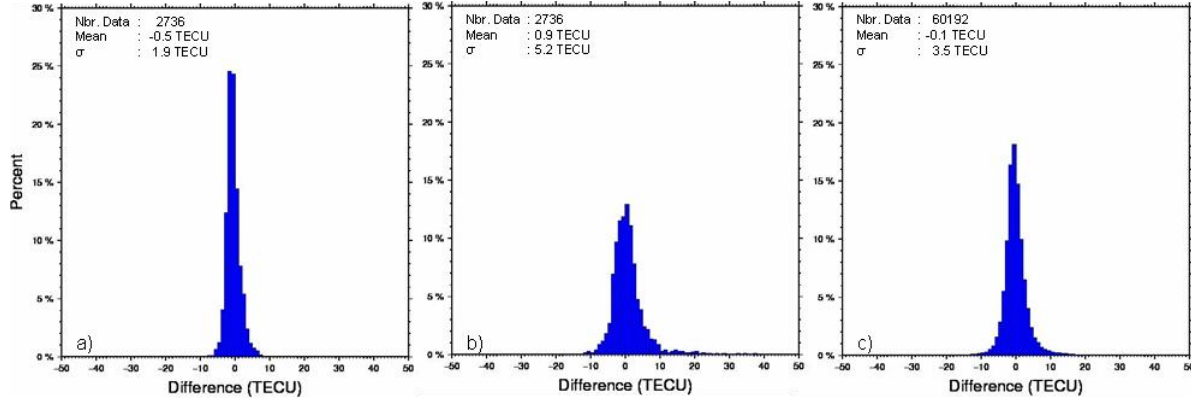
Figure 5: Differences between CODE and our estimation of TEC for a) normal day of ionospheric activity (day 292, 2003), b) geomagnetic super-storm period (day 303, 2003) and c) the entire period 292-303 2003.

4. Residuals from the L4 combination

The regional TEC maps computed in this paper only model the static-component ("*frozen*") of the ionosphere and do not include small-scale variations in the ionospheric activity. Consequently, we choose to investigate the residual ionospheric effect that is not modelled by the regional maps from the 5-min residuals of the *geometry-free* linear combination in order to improve the time and spatial resolution of the monitoring of the ionospheric activity.

The *geometry-free* (L4) observables contain principally ionospheric information. When we estimate the static-component of the ionosphere (see section 2.1) the L4 residuals are considered as noise corresponding to short-term variations in the ionospheric state. During the geomagnetic super-storm, the residuals are significantly larger (above 2m) compared to normal ionospheric activity (Figure 6).
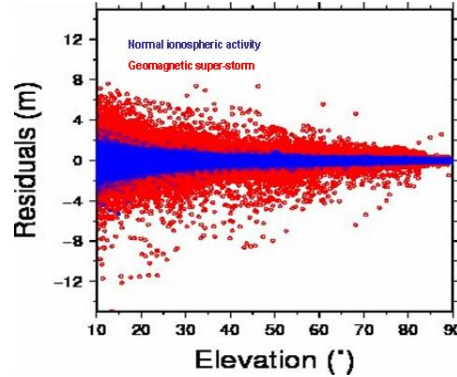

Figure 6: Residuals of the L4 linear combination (~150 GPS station) as a function of the satellite elevation. Red: geomagnetic storm; Bleu: normal ionospheric activity

The L4 residuals from different GPS stations and satellites have been used to compute the pierce points of the satellite/receiver vectors at a 450km altitude (770 pierce points each 5-minutes in 2003). The residual maps in Figure 7 highlight a spatial and temporal correlation between residuals from different satellite/receiver pairs. Some regions show small ionospheric structures not modelled in the static-component of the ionosphere (see Figure 4). A latitudinal profile through the residuals (Figure 8) shows a clear pattern around 50-55° latitude which can be interpreted as small variations in the ionospheric state.
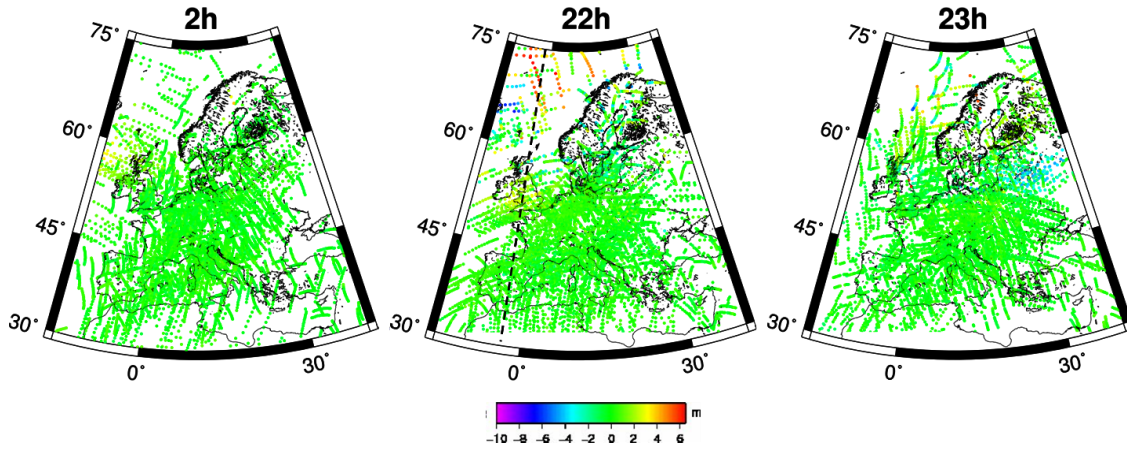
Figure 7: Residuals of the L4 linear combination (~150 GPS stations) at 2h, 22h and 23h during the geomagnetic super-storm (day 303, 2003). Each map integrates 1 hour of residuals estimated each 5 min.
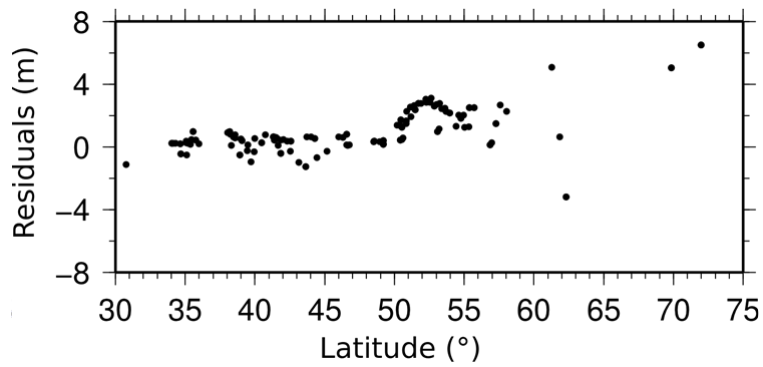
Figure 8: Profile between -6 and -2° longitude, 21h55 to 22h05 UT (dashed line on figure 6). Eight satellites (PRN 2,3,11,15,16,23,28) are visible during this period.

Presently, the EPN is composed of ~200 GPS stations. The increasing densification of the network allows estimating today 1270 pierce points each 5-minutes (Figure 9). Consequently, the coverage of the residual maps will permit to better detect small variations in the ionospheric activity over the Europe.
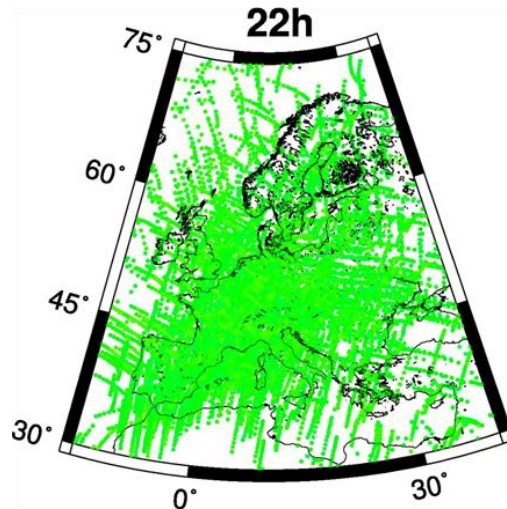
Figure 9: Residuals map at 22h for day 003 of 2008.

Conclusion

In this study, we showed that for stations close to the maximum of a large ionospheric disturbance, the estimated GPS kinematic positions from double difference ionosphere-free observables show a large degradation. This degradation is significant for many scientific applications.

The EPN data allows producing hourly TEC maps (which agree globally with the CODE products at 1 TECU level) on a one degree grid. Thanks to these TEC maps abnormal ionospheric activity related to sunspot activity can be detected. However, such a product does allow to evidence rapid changes and small-scale variations in the ionosphere. We showed that the residual maps from the zero-difference *geometry-free* linear combination can provide supplementary information on the ionospheric state. We observe spatial and temporal correlations in the residuals. Such maps will, with the increasing number of stations in the EPN, be useful to monitor the ionosphere. We are investigating optimal ways to correct kinematic positioning from higher order ionospheric effects. The residuals of the zero-difference *geometry-free* observable are the best candidate for such application.

References

Dach, R., U. Hugentobler, P. Fridez and M. Meindl, *Bernese GPS Software Version 5.0*, Astronomical Institute, University of Bern, 612p, 2007

Pulkkinen, A., S. Lindahl, A. Viljanen, and R. Pirjola, *Geomagnetic storm of 29–31 October 2003: Geomagnetically induced currents and their relation to problems in the Swedish high-voltage power transmission system*, Space Weather, 3, S08C03, doi:10.1029/2004SW000123, 2005

Schaer, S., M. Rothacher, G. Beutler and T.A. Springer: *Daily Global Ionosphere Maps Based on GPS Carrier Phase Data Routinely Produced by the CODE Analysis Center*, 1996 IGS Workshop, NOAA, Silver Spring, Maryland, USA, March 19-21,1996

Schaer, S., W. Gurtner and J. Feltens, *IONEX: The IONosphere Map EXchange Format Version 1*, February 25, 1998, in Proceedings of the 1998 IGS Analysis Centres Workshop, ESOC, Darmstadt, Germany, February 9-11, 1998, pp. 233-247.